*Progress In Electromagnetics Research*, PIER 69, 145–160, 2007

# DIRECTION OF ARRIVAL ESTIMATION METHOD USING A 2-L SHAPE ARRAYS ANTENNA

**F. Harabi, H. Changuel, and A. Gharsallah**

Groupe d'Electronique
Laboratoire de Physique de la Matière Molle
Faculté des Sciences de Tunis
El-Manar 2092 Tunisie

**Abstract**—The paper presents a new algorithm for a 2-dimensionnal direction of arrival estimation. Based on the extended Kalman filter (EKF), we analyse a recursive procedure for 2-dimensional directions of arrival (DOA) estimation and we will employ the two-L-shape arrays. A new space-variable model which we call a spatial state equation is presented using array element locations and incident angles. In this paper we briefly recapitulate the most important features of the extended Kalman filter (EKF). The performance of the proposed approach is examined by a simulation study with three signals model. The simulation results show a good estimate performance.

## 1. INTRODUCTION

The technique for estimating the parameters of multiple waves provides a convenient tool for the analysis of multiple-waves fields and eventually for actual applications to mobile communications. Therefore, we should estimate the Direction of Arrival (DOA) of highly coherent waves like desired wave and the delay waves. The high resolution DOA estimation algorithm using array antenna is attracted attention to achieve these demands.

The problem of estimating the two-dimensional directions of arrival (DOAs), namely, the azimuth and elevation angles, of multiple sources was the topic of several researches [2, 3, 7, 9], and we will employ the two-L-shape arrays that showed [12] better performances than the one L-shape [3], linear array [4–5], planar array [6–7], and the parallel shape arrays [8].

In this paper the detection and estimation of the parameters of multiple waves are discussed. Especially in the mobile communication domain in the range of $[70°, 90°]$. We will present a method for estimating the elevation and azimuth arriving waves based on the extended Kalman filter [13–15].

The general characteristics of a Kalman filter such as most-likelihood and convergence have been discussed in several papers [13–16]. On the contrary, we derive a suitable space-variable model in the present paper which we call a spatial state equation using array element locations and incident angles. Simulation results show the performance of our method even at low SNRs. With this new method we can avoid the case where both of elevation and azimuth angles are complex at the same time.

The rest of the paper is organized as follows: The data model, geometrical considerations and the new spatial state equation for incident waves are presented in Section 2, in Section 3, the extended Kalman filter is recapitulated, Section 4 presents the 2-D direction of arrival estimation algorithm, Section 5 shows simulation results and Section 6 makes conclusions.

## 2. DATA MODEL

Consider the two-L-shape uniform linear array (ULAs) in the $x$-$z$ and the $y$-$z$ planes shown in Fig. 1 with inter-element equals $d$, using three array elements placed on the $x, y$ and $z$ axes. Each linear array consists of $N$ elements. The element placed at the origin is common for referencing purposes.

Suppose that there are $K$ narrow band sources, $s(t)$, with the same wavelength $\lambda$ impinging on the array, such that $k$th source has an elevation angle $\theta_k$ and an azimuth angle $\phi_k$, $k = 1, \ldots, K$.

We put the complex base-band representation of the signal received by the $n$th element of one subarray as $y(n)\,(n = 1, 2 \ldots N)$, the signal sources are far apart from the subarray. The received vector at the nth element position is then given by:

$$y(n) = \sum_{k=1}^{K} a_n\left(\theta_k, \phi_k\right) s_k(t), \quad n = 1, 2, \ldots, N \tag{1}$$

Where $a_n\left(\theta_k, \phi_k\right)$ is the steering vector defined by:

$$a_n\left(\theta_k, \phi_k\right) = \exp\left(-j\varphi_{k,n}\right) \tag{2}$$

with $\varphi_{k,n}$ depends on the position and the geometry of the subarray showed in Fig. 1. Let us introduce the following notation:

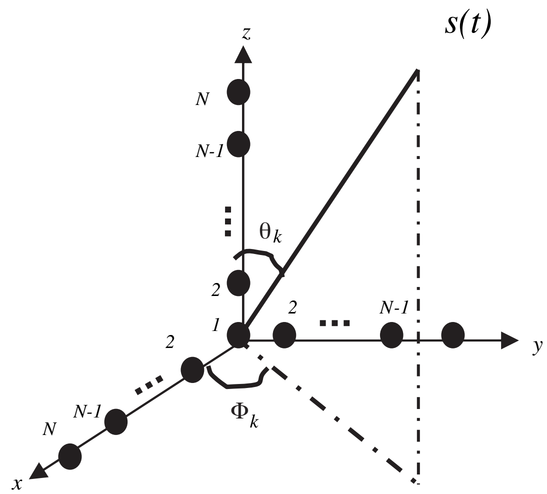


**Figure 1.** The 2-L-shape array configuration used for the joint azimuth and elevation $(\theta, \phi)$ DOA estimation.

$$
\begin{aligned}
x_{1,n} &= s_1(t)a_n(\theta_1, \phi_1) \\
x_{2,n} &= s_2(t)a_n(\theta_2, \phi_2) \\
\ldots & \\
x_{K,n} &= s_K(t)a_n(\theta_K, \phi_K)
\end{aligned}
$$

Using these notations, we can express the incident wave vector $X(n)$ at the $n$th element position as follows:

$$X(n) = [x_{1,n}x_{2,n} \ldots x_{K,n}]^T \tag{3}$$

where "$T$" denotes the transpose. Then the received signal is given by:

$$y(n) = HX(n) + \eta(n) \tag{4}$$

where $\eta$ is a complex white noise value with mean zero and covariance $\sigma^2$. $H = [11 \ldots 1]$ with $K$-components.

At the $(n + 1)$th element position, the incident wave vector is derived from that at the $n$th element position by:

$$X(n + 1) = A(\theta, \phi)X(n) \tag{5}$$

where

$$\theta = [\theta_1, \theta_2, \ldots, \theta_K], \qquad \phi = [\phi_1, \phi_2, \ldots, \phi_K]$$

$$A(\theta, \phi) = \begin{bmatrix} a(\theta_1, \phi_1) & & 0 \\ & \cdots & \\ 0 & & a(\theta_K, \phi_K) \end{bmatrix} \quad (6)$$

Equation (5) could be called a spatial state equation and Equation (4) the measurement equation.

## 2.1. Geometrical Consideration of the Steering Vector

### *2.1.1. The Steering Vector of the $z$ Axes Subarray*

We will use the $z$ axes subarray of the 2-L shape arrays antenna only to estimate the elevation angles of sources, Let $y_z(n)$ be the signal received at the linear subarray in the $z$ axes at the $n$th element.

$$y_z(n) = \sum_{k=1}^{K} a_{nz}(\theta_k)\, s_k(t) + \eta_z(n) \quad (7)$$

where the steering vector of the $z$ axes subarray is given by:

$$a_{nz}(\theta_k) = \exp\left(-j\varphi_{zk,n}\right) \quad (8)$$

and

$$\varphi_{zk,n} = \frac{2\pi(n-1)d\cos\theta_k}{\lambda} \quad (9)$$

$\theta_k$ is the elevation angle of the $k$th source signal. $\eta_z(t)$ is the additive White Gaussian noise of the $k$th source signal in the $z$ axes at the nth element.

### *2.1.2. The Steering Vector of the $x$ Axes Subarray*

In the same way, we use the $x$ axes to estimate the $x$-component of the azimuth angle. Then let $y_x(n)$ be the signal received at the linear subarray in the $x$ axes at the nth element.

$$y_x(n) = \sum_{k=1}^{K} a_{nx}(\theta_k, \phi_{kx})\, s_k(t) + \eta_x(n) \quad (10)$$

where the steering vector of the $x$ axes subarray is given by:

$$a_{nx}(\theta_k, \phi_{kx}) = \exp\left(-j\varphi_{xk,n}\right) \quad (11)$$

and

$$\varphi_{xk,n} = \frac{2\pi(n-1)d\sin\theta_k\cos\phi_k}{\lambda} \quad (12)$$

*2.1.3. The Steering Vector of the y Axes Subarray*

To estimate the $y$-component of the azimuth angle we use the $y$ axes subarray. Then let $y_x(n)$ be the signal received at the linear subarray in the $y$ axes at the nth element.

$$y_y(n) = \sum_{k=1}^{K} a_{ny}\left(\theta_k, \phi_{ky}\right) s_k(t) + \eta_y(n) \tag{13}$$

where the steering vector of the $y$ axes subarray is given by:

$$a_{ny}(\theta_k, \phi_{ky}) = \exp\left(-j\varphi_{yk,n}\right) \tag{14}$$

and

$$\varphi_{yk,n} = \frac{2\pi(n-1)d\sin\theta_k \sin\phi_k}{\lambda} \tag{15}$$

## 2.2. A New Spatial State Equation for Incident Waves

The elements of $X, A$ and $y$ are all complex in general. We reformulate the problem involving complex quantities in terms of real quantities, in order to carry out the parameter estimation of incident waves. Let the real and the imaginary parts of $x_{1,n}$ be denoted by $z_1$ and $z_2$ respectively, and the real and imaginary parts of $e^{-j\varphi_1}$ be denoted by $\alpha_1$ and $\alpha_2$, respectively. Continuing in this manner we have

$$x_{k,n} = z_{2k-1,n} + jz_{2k,n} \tag{16}$$

$$\exp\left(-j\varphi_k\right) = \alpha_{2k-1} + j\alpha_{2k} \tag{17}$$

It follows that the $L$-component complex vector $X(n)$ can be completely represented by the following real vector $X_r(n)$ with $2L$-components

$$X_r(n) = [z_{1,n}\ z_{2,n} \ldots z_{2k-1,n}\ z_{2k,n}]$$

In this way, we can rewrite (5) in terms of real vector as:

$$X_r(n+1) = A_r(\alpha)X_r(n) \tag{18}$$

$A_r(\alpha)$ is a $2L \times 2L$ square matrix, correspondingly, (4) can be rewritten as:

$$Y_r(n) = H_r(n)X_r(n) + N_r(n) \tag{19}$$

where

$$Y_r(n) = \left[\mathrm{Re}\left(y(n)\right)\ \ \mathrm{Im}\left(y(n)\right)\right]^T \tag{20}$$

$$H_r = \begin{bmatrix} 1 & 0 & 1 & 0 & \ldots & 1 & 0 \\ 0 & 1 & 0 & 1 & \ldots & 0 & 1 \end{bmatrix} \tag{21}$$

$$N_r(n) = \left[\mathrm{Re}\left(\eta(n)\right)\ \ \mathrm{Im}\left(\eta(n)\right)\right]^T \tag{22}$$

## 3. THE EXTENDED KALMAN FILTER (PREVIOUS WORK)

The Kalman filtering approach for a non linear system is based on the first order linearization of a non linear state equation using a previous estimate as the centre of the updated linear Taylor approximation. The nonlinear system is given by

$$X(n+1) = f(n, X(n)) + W(n) \tag{23}$$

$$y(n+1) = h(t, X(n)) + \eta(n) \tag{24}$$

wheredenotes the state vector (5), $Y(n)$: the measurement vector (3), $W(n)$: the process noise, $\eta(n)$: the measurement noise and $f(.)$ and $h(.)$ are nonlinear differentiable matrix functions. $W(n)$ and $\eta(n)$ are vectors with white Gaussian random elements of zero mean, and their covariance matrices are $Q$ and $R$, respectively:

$$\begin{aligned} Cov\left(W(n)W(n)^T\right) &= Q \\ Cov\left(\eta(n)\eta(n)^T\right) &= R \end{aligned} \tag{25}$$

The extended Kalman filter is described by the following equations:

$$\hat{X}(n+1/n) = f\left(n, \hat{X}(n)\right) \tag{26}$$

$$\hat{X}(n/n) = \hat{X}(n/n-1) + K(n)\left[y(n) - h\left(n, \hat{X}(n)\right)\right] \tag{27}$$

$$\begin{aligned} K(n) = {} & P(K/K-1)\prod\left(n, \hat{X}(n/n-1)\right)^T \\ & \left[\prod\left(n, \hat{X}(n/n-1)\right)P(n/n-1)\right. \\ & \left.\prod\left(t, \hat{X}(n/n-1)\right)^T + R\right]^{-1} \end{aligned} \tag{28}$$

$$\begin{aligned} P(n/K) = {} & P(n/n-1) - K(n) \\ & \prod\left(n, \hat{X}(n/n-1)P(n/n-1)\right) \end{aligned} \tag{29}$$

$$P(n/n+1) = F\left(n, \hat{X}(n/n)\right)P(n/n)F\left(n, \hat{X}(n/n)\right)^T + Q \tag{30}$$

where $\hat{X}(n/n)$ and $\left(\hat{X}(n/n-1)\right)$ denote the conditional mean estimates of $\hat{X}(n)$, based on the measurements $Y(n)$ and $Y(n-1)$, respectively. $F\left((n, \hat{X}(n/n)\right)$ and $\prod\left((n, \hat{X}(n/n-1)\right)$ denote the following Jacobian matrices evaluated at the values of $\hat{X}(n/n)$ and

$\hat{X}(n/n-1)$, respectively. $K(n)$ denotes the Kalman gain matrix. $P(n/n)$ and $P(n/n-1)$ denote the estimation error covariance matrices.

The above extended Kalman filter can also be used to estimate unknown parameters in a linear system. In the following, we apply it for Equations (26) and (27) to estimate both of elevation and azimuth angles in different subarray.

## 4. THE 2-D DIRECTION OF ARRIVAL ESTIMATION ALGORITHM

### 4.1. The Extended Kalman Filter Algorithm

The problem to estimate the elevation angle $\theta_k$ and the azimuth angle $\phi_k$ in (1) or $\alpha_{2k-1}$ and $\alpha_{2k}$ in (17), can be solved with the same procedure as parameters estimation in linear systems. We should apply an extended Kalman filter approach by means of spatial state equations of the incident waves as mentioned above. The procedure is summarized as follows:

1) Defining a space-variable vector expressing the incident waves, to obtain a spatial state equation of the incident waves. The matrix $A_r(\alpha)$ and $X_r(n)$ in (18) and $H_r$ and $Y_r(n)$ in (19), respectively, are defined.
2) Extending the state vector by including the unknown incident angles in the state vector.
3) Using the nonlinear state equation, the extended Kalman filter (26)–(30) is carried out to obtain the estimation of the elevation or the azimuth arrival waves.

Correspondingly, $F(t, \hat{X}(n/n))$ with $4L \times 4L$ size and $\prod(n, \hat{X}(n/n-1))$ with $2 \times 4L$ size, are given in more detailed from as (31) and (32).

$$\prod\left(n, \hat{X}(n/n-1)\right) = \begin{bmatrix} 1 & 0 & 1 & \dots & 1 & 0 & 0 & 0 & \dots & 0 \\ 0 & 1 & 0 & \dots & 0 & 1 & 0 & 0 & \dots & 0 \end{bmatrix} \quad (31)$$

$$F\left(t,\hat{X}(n/n)\right)=\begin{bmatrix} \hat{\alpha}_1 & -\hat{\alpha}_2 & & 0 & \hat{z}_1 & -\hat{z}_2 & & 0 \\ \hat{\alpha}_2 & \hat{\alpha}_1 & & & \hat{z}_2 & \hat{z}_1 & & \\ & \ddots & \hat{\alpha}_{2L-1} & -\hat{\alpha}_{2L} & & \ddots & \hat{z}_{2L-1} & \hat{z}_{2L-1} \\ 0 & & \hat{\alpha}_{2L} & \hat{\alpha}_{2L-1} & 0 & & \hat{z}_{2L-1} & \hat{z}_{2L-1} \\ 0 & 0 & 0 & 0 & 1 & & & 0 \\ 0 & 0 & 0 & 0 & & \ddots & & \\ 0 & 0 & 0 & 0 & & & \ddots & \\ 0 & 0 & 0 & 0 & 0 & & & 1 \end{bmatrix} \tag{32}$$

### 4.2. The 2D Direction of Arrival Estimation

The azimuth angle estimation $\hat{\phi}_k$ can be written [8] as:

$$\hat{\phi}_k = \begin{cases} \frac{1}{2}\left(\hat{\phi}_{kx}+\hat{\phi}_{ky}\right) & \text{if both } \hat{\phi}_{kx} \text{ and } \hat{\phi}_{ky} \text{ are real} \\ \hat{\phi}_{kx} & \text{if } \hat{\phi}_{ky} \text{ is complex} \\ \hat{\phi}_{ky} & \text{if } \hat{\phi}_{kx} \text{ is complex} \\ \text{Failure} & \text{if both are complex} \end{cases} \tag{33}$$

Note:

With the new spatial state equation in Section 2.2 we can avoid the case where both of elevation and azimuth angles are complex at the same time. So there are not failures, what is proved in the simulation results. We give the procedure to estimate the elevation and the azimuth angles in the flowchart of Fig. 2.

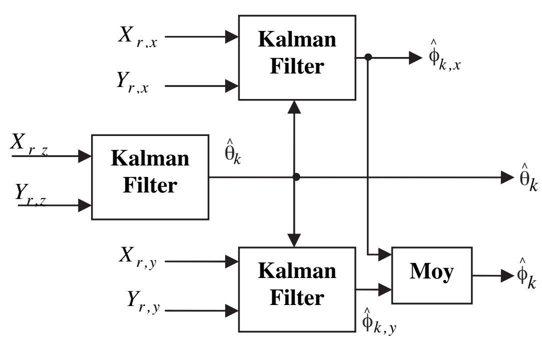


**Figure 2.** Proposed two L-shape array flowchart for the joint elevation and azimuth DOA estimation.

## 5. SIMULATION RESULTS

Computer simulations have been conducted to evaluate the 2-D DOA estimation performance of the proposed method. The parameters used in the simulation are as follows:

The sensors displacement $d$ is taken to be half the wave length of the signal waves. The incident waves are three waves $K = 3$, with directions of arrival DOA $(\theta_k, \phi_k)$, $k = 1 \dots K$. The additive noise is white Gaussian processes.

All the waves are assumed to be direct waves and the power levels are a constant 2, 3.2 and 5, respectively. The measurement noise $\eta(t)$ in (24) is assumed to be 0.1. The process noise $W(t)$ is assumed to be zero as the state (23) represents the elements state at the same time. The convergence of estimated values of the elevation and azimuth angles are plotted in Fig. 3 and Fig. 4, respectively. The abscissa is the number of iterations, and means the numbers of necessary elements.

In Figs. 3(a) and (b) the waves are located at $(60°, 20°)$, $(70°, 30°)$ and $(80°, 40°)$, respectively and signal to noise ratio (SNR)=10 dB. This is an example of the most common case because the incident angles differences are medium and, accordingly, the convergence is not bad. It is shown that the estimated values steadily converge to the actual values. About 80 iterations are required to achieve a steady state for the elevation angles. In other words, 80 out of 250 elements for the $z$ axes array are used for convergence. For the azimuth angles, only 50 iterations are required to obtain the convergence to the real azimuth angles.

In Figs. 4(a) and (b), three waves are located at $(70°, 20°)$, $(74°, 24°)$ and $(78°, 28°)$, respectively. Despite the proximity of the elevation and azimuth angles, the convergence characteristics of angles estimations show no degradation from Fig. 3. Although the variations of the elevation angles are larger and the convergence speeds are slower than in Fig. 3, the estimates errors are quite small after achieving the convergence state after 116 iterations for both azimuth and elevation angles.

Figs. 5(a) and (b) show the histogram plots for the joint elevation and azimuth angles, respectively, for a single source with DOA located at $(90°, 40°)$ by using the extended kalman filter of the 2-L shape array. We observe that the method gives close azimuth DOA estimation and the clear peaks appear around $(40°)$, but, for the elevation angle located at $(90°)$, we observe a considered estimation error. It is clear that the proposed algorithm improves performance significantly for the azimuth angle, but not for the elevation angle located at $90°$.

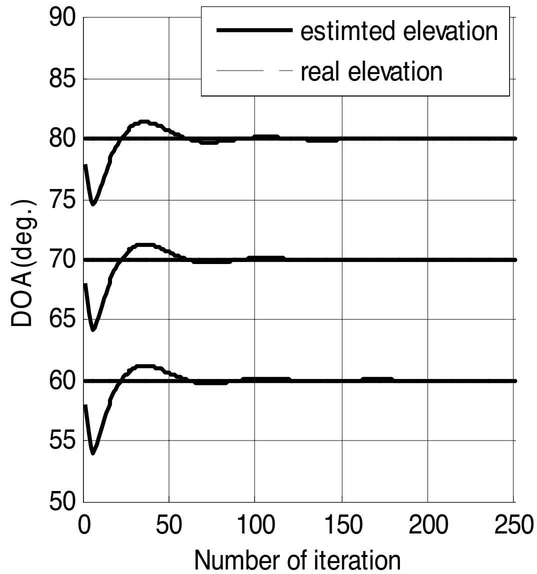


(a)

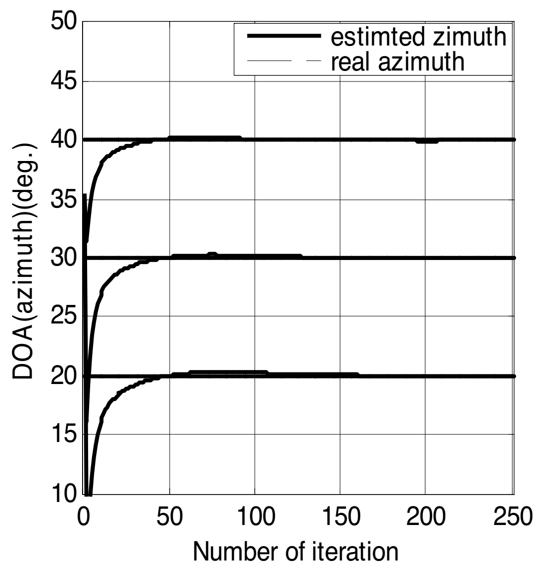


(b)

**Figure 3.** Convergence results for the sources located at $(60°, 20°)$, $(70°, 30°)$ and $(80°, 40°)$, respectively (a) Elevation angles. (b) Azimuth angles.

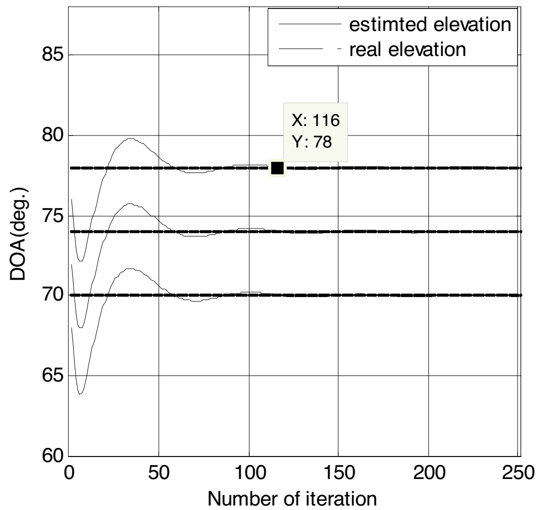


(a)

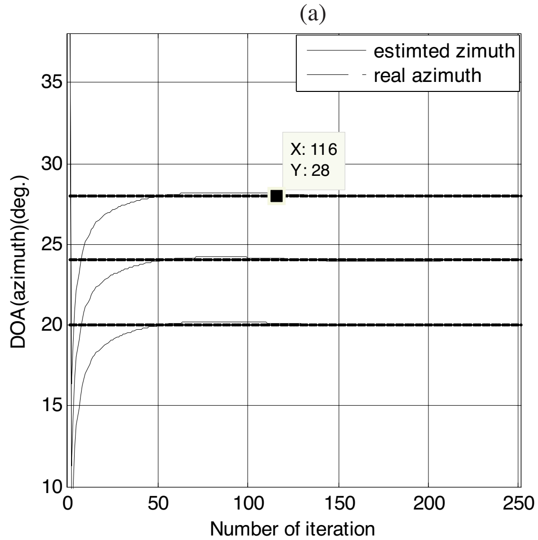


(b)

**Figure 4.** Convergence results for the sources located at $(70°, 20°)$, $(74°, 24°)$ and $(78°, 28°)$, respectively. (a) Elevation angles. (b) Azimuth angles.

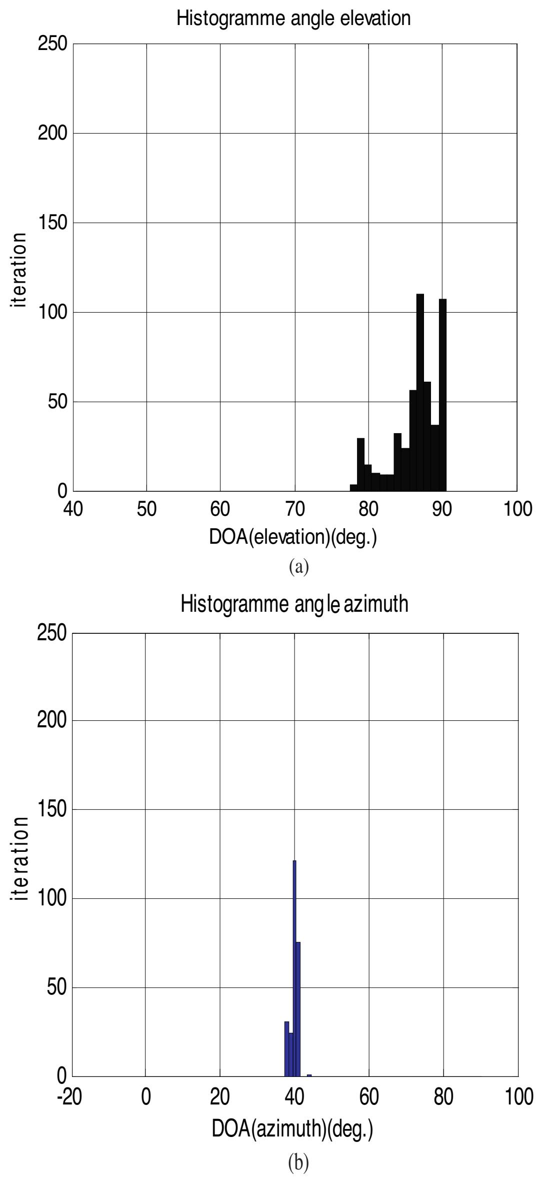


**Figure 5.** Histogram of elevation DOA estimations for a single source of DOA at $(90°, 40°)$, (a) Elevation angles. (b) Azimuth angles.

Fig. 6 shows the speed of convergence of elevation angles in the mobile communication range, which is $[70°, 90°]$, with different wave lengths from $\lambda/8$ to $\lambda$. it clear that a large number of iterations are asked when the angle of elevation approaches to 90° for all lengths of waves used. For the other cases, an acceptable convergence speed is gotten for a wave length superior or equal to $\lambda/2$.

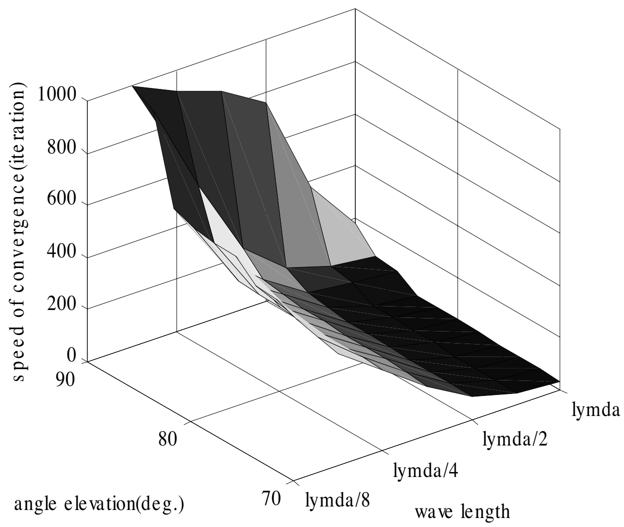


**Figure 6.** Speed of convergence of elevation angles in the mobile communication range with different wave lengths.

Fig. 7 denotes the worst convergence case where the first and the second waves are located at 0° and 90° respectively. The wave located at $(0°, 40°)$, shows good convergence characteristics but with degradation of the convergence speed, indeed we attain the real direction after 100 iterations. But the second wave located at $(90°, 40°)$ have significant errors which are 8°.

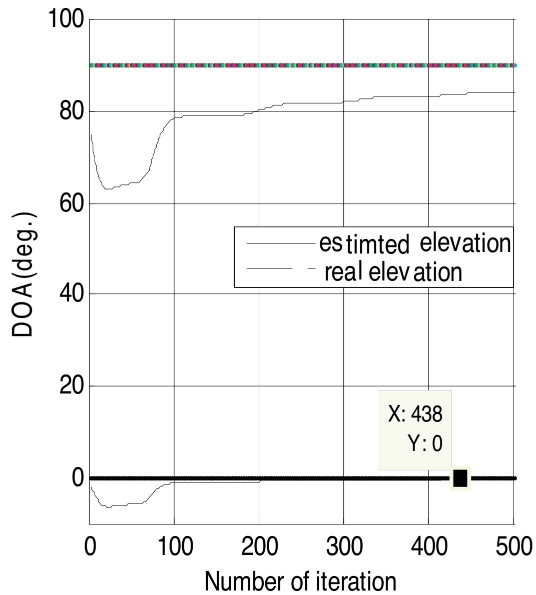


**Figure 7.** Estimated elevation angles convergence results for sources located at $(90°, 40°)$ and $(0°, 40°)$ respectively.

## 6. CONCLUSION

An antenna array configuration was proposed using the extended kalman filter method, for the 2-D azimuth and elevation angle estimation problem. The results obtained are summarized as follows.

A space variable model, called spatial state equation is derived, using the elements array of the 2-L shape antenna. We show that the extended kalman filter algorithm, which can be applied to all array configurations, is simple and applicable to practical cases. The proposed scheme reduces the estimation error of both the azimuth and elevation angles and it shows a good performance at low SNRs and at the proximity of the waves. It should be noted that the idea of the proposed approach is different from the well-known MUSIC or the PM algorithms. The angles of the arrival waves are directly estimated from the signal received at each array element, though MUSIC and PM algorithms obtain the estimation based on the spectral analysis techniques. We can also note that the performance of the proposed approach is not affected by the change of the incident waves during the computing time of the algorithm, because the signals at each array element are collected at the same sampling time.

## ACKNOWLEDGMENT

The authors gratefully acknowledge the contributions of reviewers and thank the anonymous reviewers for their valuable comments that significantly improved the presentation of this paper

## REFERENCES

1. Welch, G. and G. Bishop, "An introduction to the Kalman filter," Department of Computer Science University of North Carolina at Chapel Hill, April 2004.
2. Krekel, P. and E. Deprettre, "A two dimensional version of matrix pencil method to solve the DOA problem," *European Conference on Circuit Theory and Design,* 435–439, 1989.
3. Hua, Y., T. K. Sarkar, and D. D. Weiner, "An L-shape array for estimating 2-D directions of wave arrival," *IEEE Trans. Antennas Propagation,* Vol. 39, No. 2, 143–146, 1991.
4. Donelli, M., S. Caorsi, F. DeNatale, M. Pastorino, and A. Massa, "Linear antenna synthesis with a hybrid genetic algorithm," *Progress In Electromagnetics Research*, PIER 49, 1–22, 2004.
5. Mouhamadou, M., P. Armand, P. Vaudon, and M. Rammal, "Interference suppression of the linear antenna arrays controlled by phase with use of Sqp algorithm," *Progress In Electromagnetics Research*, PIER 59, 251–265, 2006.
6. Sotiriou, A. I., P. K. Varlamos, P. T. Trakadas, and C. Capsalis, "Performance of a six-beam switched parasitic planar array under one path rayleigh fading environment," *Progress In Electromagnetics Research*, PIER 62, 89–106, 2006.
7. Liu, T. H. and J. M. Mendel, "Azimuth and elevation direction finding using arbitrary array geometries," *IEEE Trans. Signal Processing,* Vol. 46, No. 7, 2061–2065, Jul. 1998.
8. Marcos, S., "Calibration of a distorted towed array using a propagator operator," *J. Acoust. Soc. Amer,* Vol. 93, 1987–1994, March 1993.
9. Li, P., B. Yu, and J. Sun, "A new method for two dimensional arrays," *Signal Processing,* Vol. 47, 325–332, December 1995.
10. Wu, Y., G. Liao, and H. C. So, "A fast algorithm for 2-D direction of arrival estimation," *Signal Processing,* Vol. 83, 1827–1831, August 2003.
11. Liu, T. and J. Mendel, "Azimuth and elevation direction finding using arbitrary array geometries," *IEEE Trans. Antenna and Propagations,* Vol. 53, No. 4, April 2005.

12. Tayem, N. and H. Kwon, "L-shape-2-D arrival angle estimation with propagator method," *IEEE Trans. Antenna and Propagation,* Vol. 53, No. 5, May 2005.
13. Kikuma, N., M. Anzai, M. Ogawa, K. Yamada, and N. Inagaki, "Estimation of direction of arrival land delay profile of multi-path waves by MUSIC algorithm for indoor radio communications," *IEICE Trans.,* Vol. J73-B-II, No. 11, 786–795, Nov. 1990.
14. Shu, C., "General two stage extended Kalman filters," *IEEE Trans. Automatic Control,* Vol. 48, No. 2, 289–293, February 2003.
15. Aidala, V., "Kalman filter behavior in bearings-only tracking application," *IEEE Transactions on Aerospace and Electronic Systems,* Vol. AES-15, No. 1, 29–39, Jan. 1979.
16. Mao, X., N. Koroleva, and A. Rodkina, "Robust stability of uncertain stochastic differential delay equation," *Syst. Control Lett.,* Vol. 35, 325–336, 1998.